

## Ion density calculator (IDC): A new efficient model of ionospheric ion densities

P. G. Richards,<sup>1</sup> D. Bilitza,<sup>2,3</sup> and D. Voglozin<sup>1</sup>

Received 21 November 2009; revised 15 April 2010; accepted 12 May 2010; published 5 October 2010.

[1] We present a new computationally efficient and accurate model of ion concentrations in the bottomside ionosphere based on the photochemistry. There has long been a need for efficient and accurate specification of ionospheric molecular ion concentrations. Incoherent scatter radars need to specify the relative ion concentrations in order to accurately determine plasma temperatures. Full physical ionospheric models are available but too costly and cumbersome for many applications. The international reference ionosphere (IRI) model is an efficient empirical model that accurately specifies the electron density but the molecular ion concentrations are based on limited data sets. Our new ion density calculator (IDC) model uses chemical equilibrium to determine all ion concentrations except the  $O^+$  density, which cannot be derived from chemical equilibrium above  $\sim 180$  km due to the increasing importance of diffusion. The IDC model overcomes this problem by using an iterative technique to solve for the  $O^+$  density given the electron density that is provided by the radar or the IRI model and the fact that the total ion concentration must sum to the electron density. This quasi-chemical model produces very good agreement with satellite measured ion densities and significantly improves electron and ion temperatures from incoherent scatter radars. It also produces good agreement with the Field Line Interhemispheric Plasma (FLIP) physical ionosphere model, which solves the continuity, momentum, and thermal equations. Comparisons with the IRI model point out the shortcomings of the most recent version, IRI-2007 in representing molecular ion densities.

**Citation:** Richards, P. G., D. Bilitza, and D. Voglozin (2010), Ion density calculator (IDC): A new efficient model of ionospheric ion densities, *Radio Sci.*, 45, RS5007, doi:10.1029/2009RS004332.

### 1. Introduction

[2] There has long been a need for improved computationally efficient calculations of ionospheric ion composition. For example, incoherent scatter radars measure the electron density but need the atomic to molecular ion concentrations to determine plasma temperatures. *Aponte et al.* [2007] and references therein summarize the various techniques to obtain ion densities from radar data. They investigated a technique to combine the precise

electron density information in the plasma line with very accurate ion line spectra to measure the F1 region molecular ion composition. Full physical ionospheric models could be used but they are too costly and cumbersome for many applications. The international reference ionosphere (IRI) empirical model is widely used to specify the molecular ion concentrations but they are based on limited data sets. In this paper, we present a new efficient photochemical model to accurately specify ionospheric ion densities.

[3] The ion density calculator (IDC) model is based on the chemistry that forms the basis of the Field Line Interhemispheric Plasma (FLIP) ionosphere model [Richards, 2001, 2002, 2004, and references therein]. The IDC model closely reproduces the ion densities from the FLIP model, which have recently been used to provide improved ion and electron temperatures from the Poker Flat Advanced Modular Incoherent Scatter Radar (PFISR)

<sup>1</sup>Department of Physics and Astronomy, George Mason University, Fairfax, Virginia, USA.

<sup>2</sup>Department of Computational and Data Sciences, George Mason University, Fairfax, Virginia, USA.

<sup>3</sup>Heliospheric Physics Laboratory, NASA Goddard Space Flight Center, Greenbelt, Maryland, USA.

that is located at the Poker Flat Research Range near Fairbanks, Alaska [Richards *et al.*, 2009].

[4] The FLIP model chemical scheme was originally developed from the Atmosphere Explorer mission but has been updated with more recent laboratory information. The IDC model solves for  $O^+(^2P)$ ,  $O^+(^2D)$ ,  $N_2^+$ ,  $O_2^+$ ,  $NO^+$ , and  $N^+$  using chemical equilibrium. The model also solves for the NO density because it is important for converting  $O_2^+$  into  $NO^+$ . Solving for the NO density requires solving for the  $N(^2D)$  and  $N_2(A)$  densities, which are important sources of NO.

[5] It is well known that the  $O^+$  ground state [ $O^+(^4S)$ ] is not in chemical equilibrium above approximately 180 km altitude where diffusion becomes increasingly important. The key insight of this paper is that, for some important applications, the electron density is measured or at least well specified empirically. Given the requirement that the total ion density must sum to the electron density and that all of the ions except  $O^+$  can be calculated from chemical equilibrium, we can iteratively solve the equation  $[e] - [O^+] - [NO^+] - [O_2^+] - [N^+] - [N_2^+] = 0$  for the  $O^+$  density. In practice, it is difficult to find a solution for  $O^+$  when it becomes a minor ion below approximately 150 km because even small errors in measured ion densities or model inputs can lead to significant difficulties in finding a solution for  $O^+$ . Under some circumstances, the calculated total molecular ion density can even be larger than the specified electron density. To avoid this problem, chemical equilibrium is used for all ions, including  $O^+$ , whenever the total calculated molecular ion density is greater than 85% of the specified electron density. This is a reasonable procedure because, under these conditions,  $O^+$  is a minor source of  $NO^+$  and  $O_2^+$  and diffusion is not very important. When all ions come from chemical equilibrium the calculated ion densities are normalized to the specified electron density to ensure smooth density profiles.

[6] In standard operating mode, the IDC model uses the thermospheric O,  $O_2$ , and  $N_2$  densities and neutral temperature provided by the Mass Spectrometer and Incoherent Scatter radar Extended (NRLMSISE-00) model [Picone *et al.*, 2002] together with a user-supplied electron density. However, for most of the validation studies in this paper the IDC model uses the measured O and  $N_2$  densities from the Atmosphere Explore-C (AE-C) satellite. For these comparisons, no calculations are performed if the measured O and  $N_2$  densities are unavailable. The NRLMSISE-00 model always provides the  $O_2$  density because  $O_2$  was not measured on AE-C. The electron, ion, and neutral temperatures are needed for calculating the many temperature dependent reaction rates. The AE-C satellite measured electron and ion temperatures but models are used to supply missing values. The model ion densities are not particularly sensitive to moderate errors in temperature because most

of the reaction rates are weak functions of temperature. The NRLMSISE-00 model also provides the  $N(^4S)$  density, which is important for calculating the NO density. However, the  $N(^4S)$  density is halved to agree better with the FLIP model calculated density and also produce better agreement between the measured and modeled NO density.

[7] The photoionization rates are calculated using the solar irradiances from the EUVAC model [Richards *et al.*, 1994]. The simple photoelectron flux model published by Richards and Torr [1983] provides the secondary ion production rates.

[8] The international reference ionosphere (IRI) model is a widely used empirical model of ionospheric parameters including electron density, electron temperature, ion composition, ion temperature and ion drift. It is the internationally recognized standard for the specification of ionospheric parameters and it was recently adopted by the International Standardization Organization (ISO) as Technical Specification TS 16547. IRI development has relied on data from all the different techniques used to measure ionospheric parameters from the ground and from space. Improvement efforts have primarily focused on electron density and temperature, because these are the parameters most often needed and requested by IRI users. There are, however, a number of applications that require accurate specification of ion densities. Examples are computations of plasma conductivity requiring electron-ion and neutral-ion collision frequencies [Takeda and Araki, 1985] and theoretical coupling studies that rely on an empirical input for their ionospheric ion composition or use IRI ion composition for starting and boundary conditions [e.g., Deng and Ridley, 2007]. IRI is also playing an important role as baseline against which the predictive skills of physics-based models are compared [Siscoe *et al.*, 2004] and as resource for educational purposes, e.g., visualization tools [Watari *et al.*, 2003].

[9] Ion composition modeling for IRI is limited by the relatively small amount of reliable composition data. Satellite in situ measurements by Retarding Potential Analyzer (RPA) or by Ion Mass Spectrometer (IMS) often do not measure all constituents of the ion gas and therefore the total ion density and ion composition cannot be determined. Calibration problems are another cause for excluding data sets from IRI modeling. Measurements from the ground by incoherent scatter radar are complicated by the fact that ion composition and plasma temperatures are determined simultaneously and therefore are not independent from each other. In fact one of the primary reasons for the development of the IDC model is the improvement of incoherent scatter data analysis with the help of a more realistic representation of the ion composition in the bottomside ionosphere.

[10] Currently, IRI provides two options for the ion composition ( $O^+$ ,  $O_2^+$ ,  $NO^+$ ) in the bottomside ionosphere.

An older model based on the work of *Danilov and Semenov* [1978] with ion mass spectrometer measurements from 43 rocket flights and a newer model (now the standard/default) by *Danilov and Smirnova* [1995] that expands on the earlier study by adding additional rocket flights and for the region above 200 km data from the AE-C, S3-1, AEROS-B, Sputnik-3 and Cosmos-274 satellites. Both models describe dependencies on solar zenith angle, season, and solar activity. For our study we use the latest version of the model, IRI-2007, with the standard ion composition and the magnetic storm model turned on. The storm model simulates the reduction in ionospheric electron density that occurs during magnetic storms. The model is available at the IRI homepage (<http://iri.gsfc.nasa.gov>) and at the Community Coordinated Modeling Center (<http://ccmc.gsfc.nasa.gov>).

## 2. Atmosphere Explorer Satellite Data

[11] The purpose of the Atmosphere Explorer (AE) mission was to investigate the thermosphere, with emphasis on the energy transfer and processes that govern its state. The study of photochemical processes accompanying the absorption of solar EUV radiation in the earth's atmosphere was accomplished by making closely coordinated measurements of most reacting constituents and the solar input. This data set is ideally suited to our study, not only because it contains most of the required measurements, but also because of its extensive verification and accessibility. The data from each instrument was summarized every 15-seconds for inclusion in a unified abstract (UA) database. A detailed description of the data including calibration techniques is available from the National Space Science Data Center (NSSDC) web site [ftp://nssdcftp.gsfc.nasa.gov/spacecraft\\_data/ae/aedoc/](ftp://nssdcftp.gsfc.nasa.gov/spacecraft_data/ae/aedoc/).

[12] Numerous studies of the ion and neutral chemistry of the upper atmosphere have benefited from the use of AE database. The AE program was a major source of data for the NRLMSISE-00 model and has also supported the development of the IRI model. In addition, the thermosphere and ionosphere chemical scheme in general use today owes much to the use of the AE data to verify the applicability of laboratory measured reaction rates to the space environment.

[13] The AE missions consisted of 3 spacecraft carrying similar instrumentation. This study uses data from the AE-C satellite that was launched 16 December 1973 into an elliptical orbit, which was altered many times in the first year of life by means of an onboard propulsion system employing a 3.5-lb thruster. The purpose of these changes was to alter the perigee height down to 129 km. After this period, the orbit was circularized and was raised periodically to about 390 km when it would decay to 250 km altitude. During the first year, the latitude of perigee moved from about 10 degrees up to 68 degrees

north and then down to about 60 degrees south. The payload on all 3 satellites included instrumentation for the measurement of solar EUV; the composition of ions and neutral particles; the density and temperature of neutral particles, positive ions, and electrons; airglow emissions; photoelectron energy spectra; and proton and electron fluxes up to 25 keV.

[14] This study uses neutral densities from the Open Source Neutral Mass spectrometer (OSS) [*Nier et al.*, 1973], the ion temperature and total ion density from the retarding potential analyzer (RPA) [*Hanson et al.*, 1973], and the electron temperature from the cylindrical electron probe (CEP) [*Brace et al.*, 1973]. The IDC model ion densities are compared to ion densities from the Bennett ion mass spectrometer (BIMS) [*Brinton et al.*, 1973] and the Magnetic Ion Mass Spectrometer (MIMS) [*Hoffman et al.*, 1973]. Comparisons are also made to the NO densities from the ultraviolet nitric oxide experiment (UVNO) [*Barth et al.*, 1973] because NO is important for converting  $O_2^+$  to  $NO^+$  below  $\sim 150$  km.

## 3. Results

[15] Most of the IDC model validation studies in this paper compare the model ion densities with ion densities measured by the AE-C satellite for magnetically quiet and disturbed periods in 1974. However, we first show that the simple IDC model accurately reproduces the FLIP model ion densities both in the daytime and nighttime. These IDC-FLIP model comparisons are done for solar maximum conditions to complement the IDC-AE-C comparisons, which are all at solar minimum. We present comparisons for specific AE-C orbits followed by statistical comparisons for the January to November 1974 period when the satellite was in a highly elliptical orbit.

### 3.1. The 16–17 March 1990 Solar Maximum IDC-FLIP Model Comparisons

[16] Figure 1 (top) shows a comparison between the IDC model (lines) and FLIP model (solid symbols) for solar maximum conditions at noon 17 March 1990. For this calculation, the IDC model takes the FLIP model electron density as input and calculates the ion and NO densities. The overall agreement between the IDC and FLIP model densities is remarkably good and the FLIP model electron density agrees well with the Millstone Hill incoherent scatter radar (open circles). The  $NO^+$  density is slightly underestimated at the highest altitudes due to the neglect of vibrationally excited  $N_2$ , which speeds up the  $O^+ + N_2 \rightarrow NO^+ + N$  reaction rate. The discrepancy would be slightly greater except that the IDC model uses the reaction rate of *Hierl et al.* [1997]. This reaction rate is not generally applicable in the

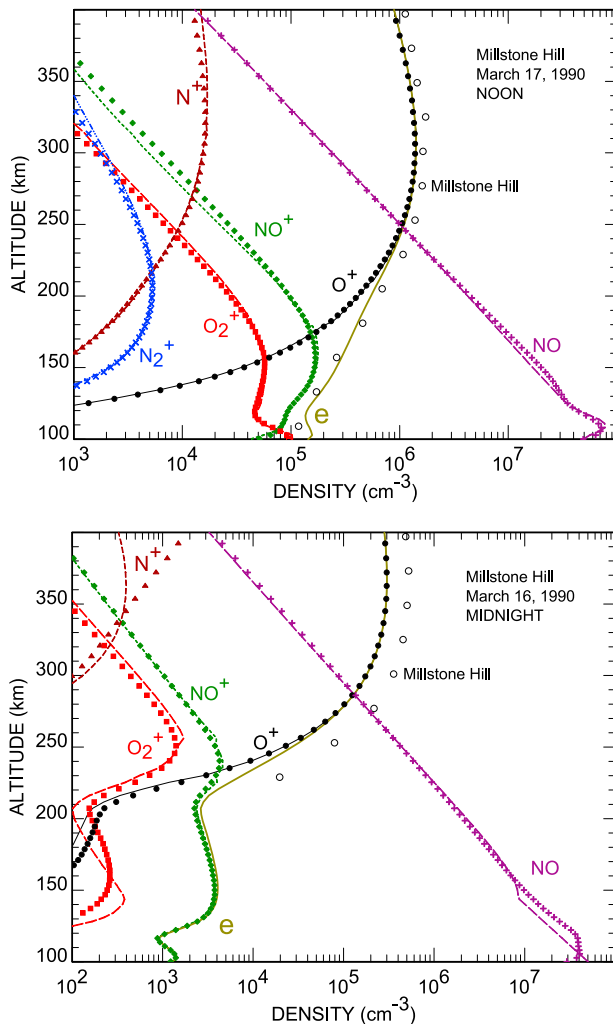


**Figure 1.** Comparison of ion and electron densities from IDC model (lines) with those from the FLIP model (solid symbols) for (top) noon 17 March 1990 and (bottom) midnight 16 March 1990. The open circles are from the Millstone Hill incoherent scatter radar. The IDC model uses the FLIP model electron densities and the NRLMSISE-00 neutral densities.

ionosphere because the rate is affected by vibrational excitation in the laboratory above 1000 K. Although  $N_2$  is vibrationally excited in the thermosphere it is not necessarily the same as in the laboratory. The FLIP model solves diffusion equations for the  $N_2$  vibrational distribution in the thermosphere but this is too cumbersome and time consuming for the IDC model. Using the reaction rate of *Hierl et al.* [1997] is a reasonable compromise.

[17] Figure 1 (bottom) shows a comparison between the IDC model (lines) and the FLIP model (solid symbols) for solar maximum conditions at midnight 16 March 1990. For this calculation, the IDC model takes the FLIP model electron density as input and calculates the ion and NO densities. The overall agreement between the IDC and FLIP model densities is remarkably good for  $O^+$ ,  $O_2^+$ , and  $NO^+$ . The IDC model underestimates the  $N^+$  density above 350 km at night due to the neglect of diffusion. The FLIP model underestimates the electron density from the Millstone Hill incoherent scatter radar (open circles) by almost a factor of 2. The nighttime ionosphere is difficult for any ionosphere model to model accurately because small errors in input parameters (winds, neutral densities, plasmaspheric fluxes) can produce large deviations in electron density as the ionosphere decays. This is not a problem in the daytime ionosphere because it is a driven system that is close to local equilibrium.

### 3.2. The 12 September 1974 Daytime Low $K_p$ AE-C Comparisons

[18] The September 1974 period has previously been studied using the FLIP model [Richards, 2002, 2004]. September 1974 was also a period of low to moderate solar activity with the daily F10.7 index ranging from 78 on 1 September and steadily rising to a peak of 106 on 13 September and then steadily declining. The 3-month average F10.7 index (F10.7A) was 91. Magnetic activity was low until a major storm occurred on 15 September.

[19] The detailed model-data single-orbit comparisons presented in this paper are for the MIMS measured ion densities, but statistical comparisons with BIMS ion densities are also shown. The RPA instrument provides a third measurement of the total ion density but does not provide individual ion densities. The three methods give different total ion density values but they generally agree within the stated instrumental errors.

[20] Figures 2a and 2b show the ion density model-data comparisons for the down leg portion of orbit 3156 on 12 September 1974 when the satellite was descending from the South Polar Region to perigee over northern Australia. The day 12 September 1974 was a magnetically quiet day following an extended period of low magnetic activity.

[21] Figure 2a shows the case when the IDC model (lines) uses the measured total ion density from the MIMS instrument (symbols) for the electron density as well as the OSS measured O and  $N_2$  density. Note that the model always uses the NRLMSISE-00  $O_2$  density because the satellite did not measure the  $O_2$  density. The IDC model used the CEP measured electron temperature and the RPA measured ion temperature, which was also adopted for the neutral temperature. As mentioned pre-

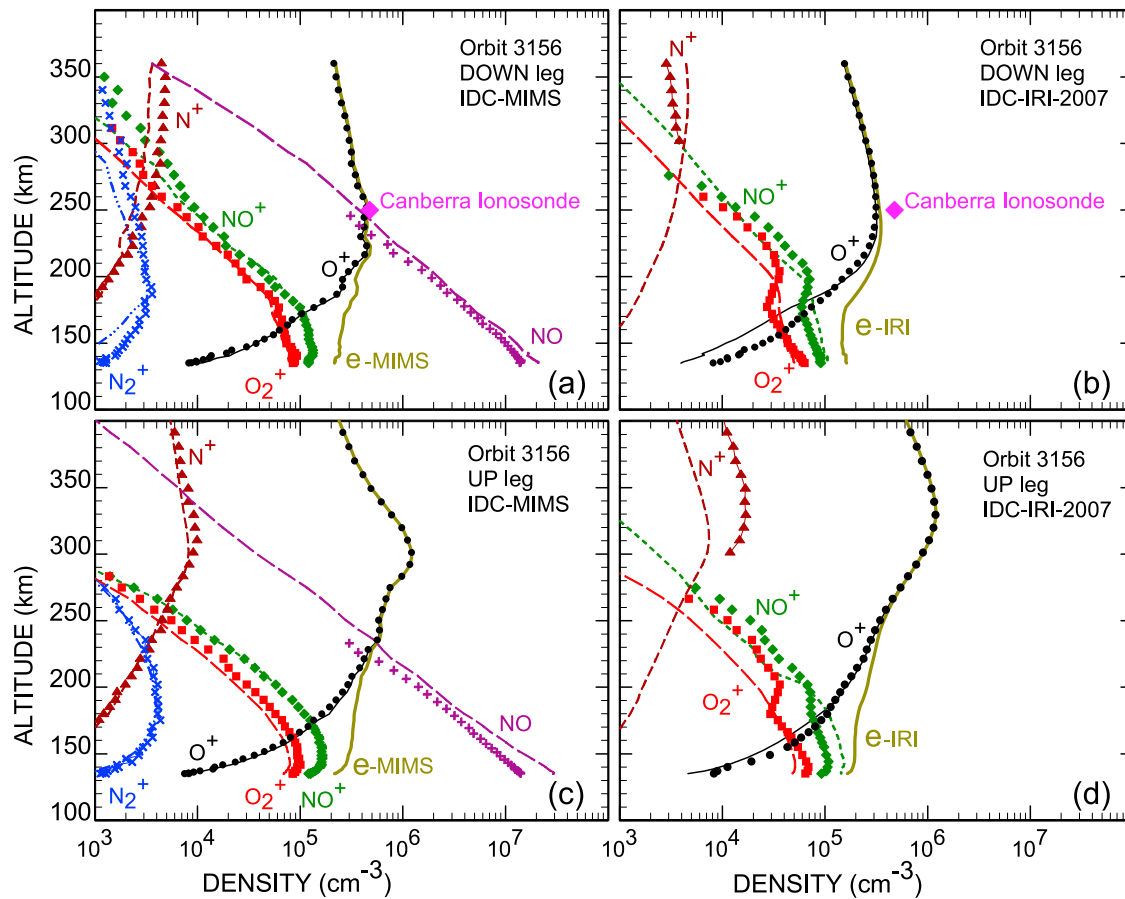


**Figure 2.** Comparison of ion and electron densities for the down leg and up leg portions of AE-C Orbit 3156 on 12 September 1974. (a) The IDC model (lines) and AE-C MIMS data (symbols) for the down leg with the IDC model using the MIMS measured electron densities and the OSS measured neutral densities. (b) The IDC and IRI model densities for the down leg with IDC using the IRI electron densities and the NRLMSISE-00 model neutral densities. (c and d) The same comparisons as Figures 2a and 2b for the up leg. The large diamond shows the  $N_m F_2$  measured by the Canberra ionosonde.

viously, the electron, ion, and neutral temperatures are needed for calculating the many temperature dependent reaction rates. There is excellent agreement between the MIMS total ion density and the peak electron density from the Canberra (35S, 149E) ionosonde (large diamond) for this orbit. The agreement between the measurements (symbols) and the IDC model (lines) in Figure 2a is very good for  $O^+$  and  $N^+$  at all altitudes and very good for molecular ions below 250 km. Above 250 km, the IDC model increasingly underestimates the MIMS molecular ion densities. However, the model agrees well with the BIMS ion densities (not shown) above 250 km on this orbit. Because there were no UVNO measurements on orbit 3156, the NO density is from orbit 3168 on the same day, which had similar altitude, latitude, and local

time but was shifted 30 degrees in longitude to the east. The ion density calculations were not done for orbit 3168 because there were no measured O or  $N_2$  densities. There is good agreement between the measured and modeled NO density.

[22] If the measured electron and neutral densities were not available, the IRI-2007 and NRLMSISE-00 densities could be used to estimate the ion composition on 12 September 1974. Figure 2b shows the ion density comparisons between the IDC model (lines) and the IRI-2007 model (symbols) when the IRI-2007 electron density and the NRLMSISE-00 model neutral densities are used for the IDC model calculations. The IRI-2007 model also supplies the electron, ion, and neutral temperatures. This would be the default model calculation in

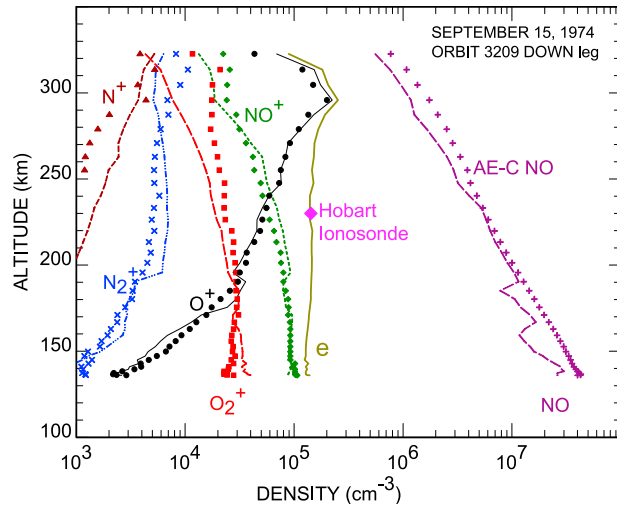


**Figure 3a.** Comparison of ion and electron densities from the IDC model (lines) and AE-C Orbit 3209 down-leg (symbols) 15 September 1974. The large diamond shows the  $N_m F_2$  measured by the Hobart ionosonde during the satellite over-flight. The IDC model uses the MIMS measured electron densities and the OSS measured neutral densities.

the absence of measured electron densities. The IRI-2007 model was evaluated at the same points along the orbit as the measurements. The IRI-2007 model electron density is a little lower than the measured total ion density but it is still a good representation. The IRI-2007 model underestimates the measured molecular ion densities below 200 km and overestimates them above 200 km. However, the main problem with the IRI-2007 model  $\text{NO}^+$  and  $\text{O}_2^+$  densities is the shape of altitude profiles. The MIMS profiles are Chapman like with a single peak below 150 km while the IRI-2007 profiles have a peak above 200 km. Similar problems with the IRI nighttime molecular ion densities have been reported by *Vlasov et al.* [2005] and *Nicolls et al.* [2006] who combined radar electron density measurements and airglow emissions and found that the IRI model overestimates the nighttime  $\text{O}_2^+$  density above  $\sim 230$  km.

[23] Above  $\sim 200$  km, the  $\text{NO}^+$  and  $\text{O}_2^+$  IDC model profiles approximately follow the scale heights of  $\text{N}_2$  and  $\text{O}_2$  respectively. This can be readily understood from the chemistry. Taking  $\text{O}^+$  as the dominant  $\text{O}_2^+$  source above 200 km,  $\text{O}_2^+$  production  $\approx k_1[\text{O}^+][\text{O}_2]$  and loss  $= k_2[\text{O}_2^+][e]$ , where  $k_1$  and  $k_2$  are reaction rate coefficients. Given that  $[e] \approx [\text{O}^+]$  above  $\sim 200$  km, then  $[\text{O}_2^+] \approx (k_1/k_2)[\text{O}_2]$ . A similar analysis applies to  $\text{NO}^+$  but it is more complicated because there are other sources. Below 200 km, the scale heights change because other sources of  $\text{O}_2^+$  and  $\text{NO}^+$

become more important. Note that below approximately 180 km, all model densities including  $\text{O}^+$  are generally obtained from chemical equilibrium because the total molecular ion density exceeds 85% of the electron density.

[24] Figures 2c and 2d show similar ion density comparisons to Figures 2a and 2b but for the up leg portion of orbit 3156 on 12 September 1974 when the satellite was ascending from perigee over northern Australia across the equator into the Northern Hemisphere. The agreement between the IDC model and the AE-C data is excellent for all ions including  $\text{N}_2^+$  and  $\text{N}^+$ . However, the IRI model problems indicated in Figure 2b are also evident in Figure 2d.

### 3.3. The 15 September 1974 Daytime High $K_p$ AE-C Comparisons

[25] Figures 3a, 3b, and 3c show ion density comparisons for the down leg portion of AE-C orbit 3209 on 15 September 1974. This was a magnetically disturbed day following an extended period of low magnetic activity. The measured peak electron density decreased by a factor of 2 from 12 September to 15 September.

[26] Figure 3a shows the comparison between the measured and modeled ion densities when the IDC model uses the measured total ion densities from the MIMS instrument for the electron density as well as the measured O and  $\text{N}_2$  densities and electron and ion temperatures. Even under these disturbed conditions, the

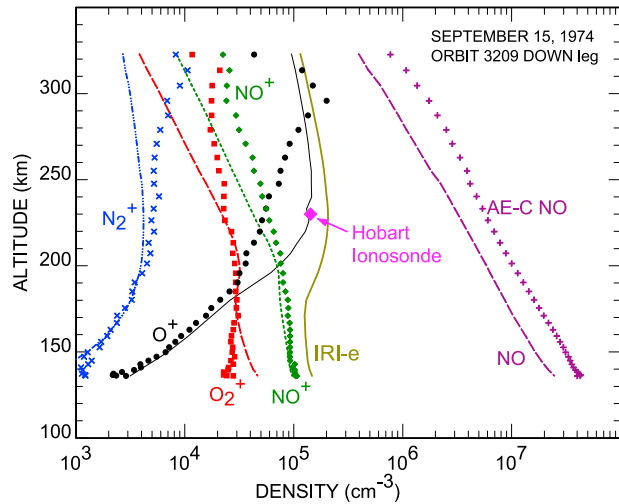


**Figure 3b.** Comparison of ion and electron densities from the IDC model (lines) and AE-C Orbit 3209 down-leg (symbols) 15 September 1974. The IDC model uses the IRI electron densities and the NRLMSISE-00 model neutral densities.

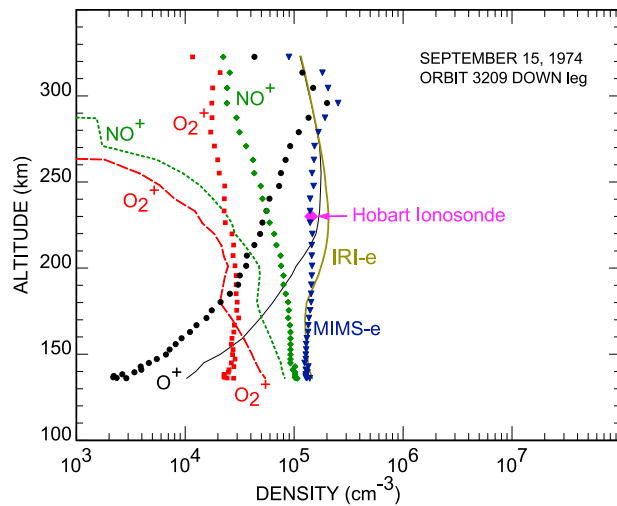


**Figure 3c.** Comparison of ion and electron densities from the IRI-2007 model (lines) and AE-C Orbit 3209 down-leg (symbols) 15 September 1974.

agreement between the measurements (symbols) and the IDC model (lines) is excellent for all ions except for  $O_2^+$  above 200 km. The  $O_2^+$  problem most likely indicates a problem with the NRLMSISE-00 model  $O_2$  density under these disturbed conditions. Indeed, the NRLMSISE-00 model O and  $N_2$  densities are considerably lower than the OSS measurements on this day [Richards, 2002]. The  $NO^+$  density is particularly well modeled at all altitudes and there is excellent agreement between the satellite total ion density and the peak electron density from the Hobart (43S, 147E) ionosonde (large diamond).

[27] There is also generally good agreement between the measured and modeled NO density, which has greatly increased compared to 12 September. The irregular NO behavior below  $\sim 180$  km is caused by irregularities in the measured ion temperatures, which were used for the neutral temperatures. The NO density is very sensitive to neutral temperature through the reaction  $O_2 + N \rightarrow NO + O$ .

[28] The main limitations on the accuracy of the IDC model ion densities during ionospheric storms are the accuracies of the IRI-2007 electron density and the NRLMSISE-00 model neutral densities. This is illustrated in Figure 3b, which shows the ion density comparisons between the IDC model (lines) and the AE-C MIMS (symbols) for 15 September 1974 when the IRI-2007 electron density and the NRLMSISE-00 model neutral densities are used for the IDC model calculations. The IRI-2007 storm model gives a factor of 1.5 reduction in peak electron density from the magnetically

quiet 12 September. The measurements show a factor of 2 reduction in peak electron density. The IDC model reproduces the  $NO^+$ ,  $O_2^+$  and  $N_2^+$  measured densities reasonably well below 200 km but greatly over estimates the  $O^+$  densities between 170 and 260 km. The NO densities are also not as well modeled primarily because the NRLMSISE-00 model neutral temperature is lower than the measured ion temperature.

[29] Despite the IDC model problems under disturbed conditions illustrated in Figure 3b, it is still far superior to the IRI-2007 model ion densities. Figure 3c shows the comparison between the AE-C measured (symbols) and IRI-2007 model (lines) ion densities for 15 September. There is poor agreement between the IRI-2007 model and the data for all ions on this magnetically disturbed day. Comparing Figure 3c with Figure 3b shows that the IDC model gives superior results although the  $O^+$  density is not satisfactory in either case because the NRLMSISE-00 model underestimates the molecular neutral densities.  $N_2^+$  and NO densities are not shown in Figure 3c because they are not available from the IRI-2007 model.

[30] Figure 4 shows the comparison of the IDC model and satellite data for the upleg portion of orbit 3209 when the satellite was ascending over the equator to the Northern Hemisphere from perigee over northern Australia. The IDC model uses the measured total ion density from the MIMS instrument for the electron density as well as the measured neutral density and electron and ion temperatures. The upleg portion of the orbit shows little evidence of magnetic disturbance, which is as expected

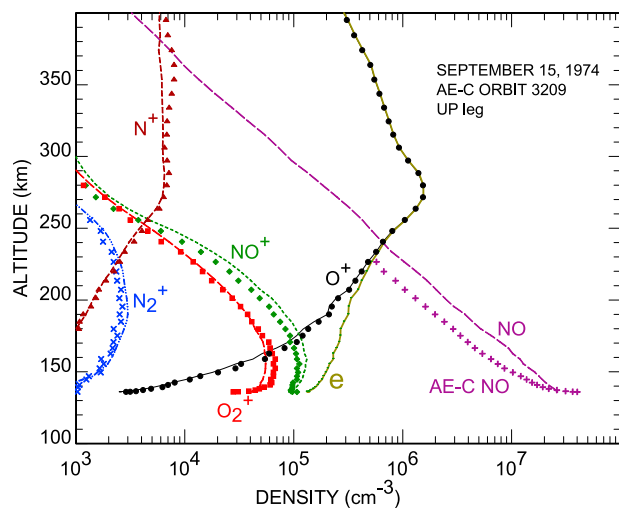


**Figure 4.** Comparison of ion and electron densities from IDC (lines) and AE-C Orbit up-leg 3209 (symbols) for 15 September 1974. The IDC model uses the MIMS measured electron densities and the OSS measured neutral densities.

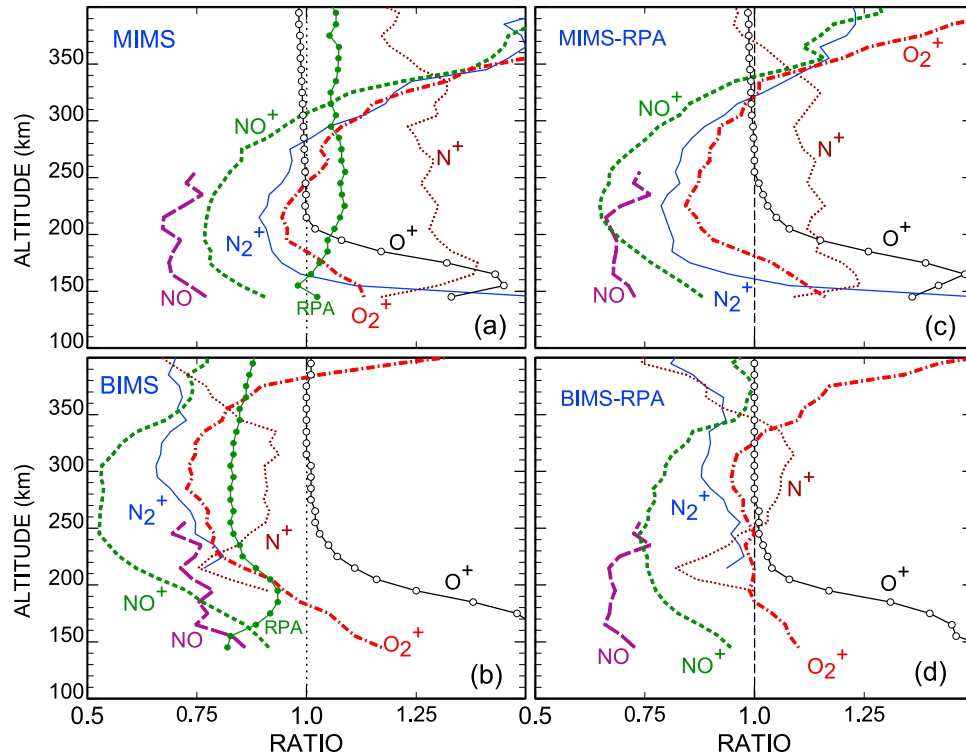


**Figure 5.** Medians of the ratios of the measured to modeled densities for all data from January to November 1974. (a) The case for the MIMS measured ion densities. (b) The case for the BIMS measured ion densities. The lines with solid circles show the ratio of the MIMS (BIMS) to RPA total densities. (c and d) The cases when the MIMS and BIMS measured ion densities are normalized to the RPA total ion density. The IDC calculations use the OSS measured O and  $N_2$  densities.

for the equatorial region. Once again, the agreement between the ion measurements (symbols) and the IDC model (lines) is excellent. The NO density is overestimated in the model.

### 3.4. All 1974 Daytime Statistical AE-C Comparisons

[31] Figure 5 shows the ratios of the measured to modeled densities for all daytime orbits from January through November 1974 when the orbit was highly elliptical. The orbit became nearly circular during December. Ratios outside the range 0.01 to 100 were eliminated from the analysis as most likely indicating a problem with either the measured ion density or the measured neutral densities and temperatures that are used as model inputs. Both medians and averages were calculated but only medians are plotted to minimize the effect of outliers. The IDC calculations use the OSS measured O and  $N_2$  densities and the NRLMSISE-00  $O_2$  densities. The *Brace and Thelis* [1978] empirical model provides Te whenever the CEP measurements are not

available. This model is based on the CEP Te measurements from AE-C and provides an accurate representation of the data. The NRLMSISE-00 model is used for the ion temperature whenever the RPA data are not available. This data selection produces approximately 60,000 data points for the ratio analysis. The data were divided into 10 km altitude bins for the analysis and bins with fewer than 100 data points were excluded from the plots.

[32] Figure 5a shows the altitude variation of the density ratios when the IDC model uses the measured total ion density from the MIMS instrument for the electron density. Figure 5b shows the same thing when the BIMS ion density is used for the electron density. The lines with solid circles in Figures 5a and 5b also show the ratio medians of the MIMS and BIMS to the RPA total ion densities. The MIMS ion densities are generally about 10% larger than the RPA ion densities while the BIMS ion densities are generally about 20% smaller than the RPA ion densities. Figures 5a and 5b show model-

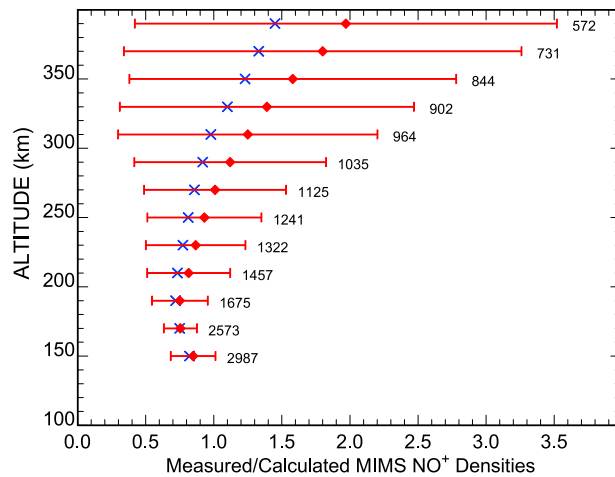


**Figure 6.** Ratio of measured to modeled MIMS  $\text{NO}^+$  densities. The crosses show the medians and the diamonds with error bars show the averages and standard deviations. The numbers adjacent to the error bars show the number of points at each altitude.

data agreement to be typically within 25% between 150 and 300 km except for the BIMS  $\text{NO}^+$  density. The  $\text{O}^+$  density ratio increases below  $\sim 200$  km where it becomes a minor ion and the model is most likely to use chemical equilibrium for all species.

[33] The RPA instrument provides a third measurement of the total ion density, which can be used for the electron density in the IDC model. Since the RPA does not provide individual ion densities, we obtained individual ion densities by normalizing the MIMS and BIMS ion densities using the RPA total ion density. The implicit assumption is that the MIMS and BIMS relative ion concentrations are correct but that the overall magnitude needs to be adjusted. This normalization has a double effect on the measured to modeled molecular ion density ratios. For example, the normalization increases the BIMS ratios by increasing the measured ion densities. It also decreases the IDC model molecular ion densities by increasing the electron recombination rate. The opposite is true for the MIMS molecular ion densities. Figures 5c and 5d show the same results as Figures 5a and 5b except that the IDC model used for the RPA electron density and the MIMS and BIMS densities have been normalized to the RPA density.

[34] It is not clear which of the three ion measurements is the most accurate. However, it may be significant that the RPA normalization brings the MIMS and BIMS ion density ratios into better agreement.

[35] The statistical results in Figure 5 show that the IDC model produces a satisfactory representation of the

data below approximately 250 km given the uncertainties in the data. The high altitude problems do not affect the usefulness of the model for applications to empirical models or radar analysis because the molecular ions are minor constituents at these altitudes. The results in Figures 5a and 5b were obtained without restriction on magnetic activity. We repeated the analysis for several different levels of  $A_p$  and there was little effect on the results.

[36] It is not clear why all the MIMS molecular ion ratios increase so much above 250 km while the BIMS  $\text{NO}^+$  and  $\text{N}_2^+$  ratios do not. The increase of the ratios with altitude could be due to the fact that low densities may be below the measurement threshold. This would skew the ratio distributions to higher values. In fact, the scatter in the ratios increases substantially with altitude. This can be seen in Figure 6, which shows the basic statistics for the ratio of measured to modeled MIMS  $\text{NO}^+$  densities. The crosses show the medians while the diamonds with error bars show the averages and standard deviations. The numbers adjacent to the error bars show the number of points for each altitude. To avoid cluttering the figures, 20 km altitude bins have been used in Figure 6 rather than 10 km bins. This coarser resolution reduces the standard deviations slightly but does not significantly change the medians and averages. Figure 6 shows that below approximately 300 km, the medians and averages are very close and the standard deviations are relatively small.

### 3.5. The 29 January 1971 Daytime Rocket Densities

[37] There are few ion density measurements below 130 km at mid latitudes because these require rocket flights. Figure 7 shows a comparison of ion densities from IDC and FLIP models (lines without symbols) with those from a rocket flight at Keweenaw, Michigan on 29 January 1971 [Aikin *et al.*, 1977]. The rocket data are displayed with lines and symbols. The local time was 14.17 and the solar zenith angle was 67 degrees. The IDC model (Figure 7, top) used the measured total ion density as the electron density and the NRLMSISE-00 model neutral densities. There is good agreement for the atomic ions but only fair agreement for the molecular ions. The instrument was unable to distinguish between  $\text{N}_2^+$  and  $\text{Si}^+$  ions so the bulge around 105 km may come from an  $\text{Si}^+$  layer. However, the rocket did measure numerous metallic ions and none of these shows a bulge near 105 km. On the other hand, the good  $\text{N}_2^+$  agreement above 115 km is evidence that there could be an  $\text{Si}^+$  layer.

[38] The FLIP model (Figure 7, bottom) produces better agreement with the measured  $\text{NO}^+$  and  $\text{O}_2^+$  densities. The better agreement with the data comes from the larger  $\text{NO}$  densities due to the inclusion of diffusion in

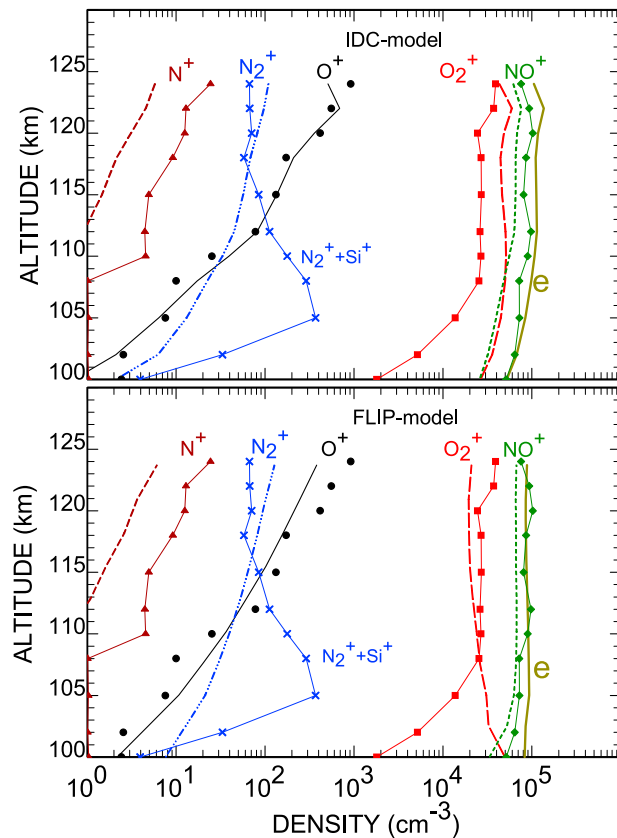


**Figure 7.** Comparison of IDC and FLIP model ion and electron densities with densities from a rocket flight at Keweenaw, Michigan on 29 January 1971 at 14.167 LT. The symbols show the data while the lines without symbols show the model values. (top) The IDC model used the rocket measured electron density and the NRLMSISE-00 model neutral densities. (bottom) The standard FLIP model calculation.

the FLIP model. Indeed, there is very good agreement above 105 km when the IDC model uses the FLIP model NO density, which is a factor of 2 larger than the IDC model density on this day. The FLIP model NO density is larger because the two previous days had very high levels of magnetic activity. The magnetic activity enhances the production of NO above 130 km and then it diffuses downward where the NO lifetime is of the order of a day. The rapid fall off of the  $O_2^+$  density below 105 km may indicate that the actual NO density is even larger than the FLIP model NO density in this region. Keweenaw is at a high enough latitude ( $L = 3.9$ ) to be affected by aurorally produced NO. There is no evidence of auroral activity at the time of the rocket flight but, as NO has a long lifetime

at these altitudes, it could have been produced earlier at this location or even transported from higher latitudes.

#### 4. Conclusions

[39] This work has demonstrated an accurate and efficient model for specifying ionospheric ion densities that is based on the photochemistry. The model accurately reproduces the ion densities from the comprehensive FLIP physical model that solves the full continuity and momentum equations. It also produces satisfactory agreement with satellite data.

[40] The accuracy of the IDC ion densities will be compromised if there is rapid convection or soft auroral particle precipitation. Moderate convection of plasma to the radar site would not affect the utility of the IDC model because the basic chemistry is unchanged. On the other hand, rapid convection is a major problem for any model because it increases the ion temperature and changes reaction rates. Auroral precipitation is not as problematic as rapid convection for the IDC model because the additional production is implicit in the measured electron density. We tested the IDC model by inputting the electron density from a FLIP model run that had auroral precipitation. The IDC model does not have auroral precipitation. There was good agreement between the FLIP and IDC models for the atomic to total molecular ion density ratio, which is the main need for the radar analysis. However, the  $O_2^+$  was relatively more abundant than  $NO^+$  in the FLIP model calculation.

[41] This model will be useful for obtaining more accurate electron and ion temperatures from incoherent scatter radars. It could be incorporated directly into the international reference ionosphere model or could be used to build a better analytical specification of the ion densities.

[42] **Acknowledgments.** This research was supported by NASA grants NNX07AN03G and NNX08AF43G to George Mason University.

#### References

- Aikin, A. C., R. A. Goldberg, W. Jones, and J. A. Kane (1977), Observations of the mid-latitude lower ionosphere in winter, *J. Geophys. Res.*, *82*, 1869–1875, doi:10.1029/JA082i013p01869.
- Aponte, N., M. P. Sulzer, M. J. Nicolls, R. Nikoukar, and S. A. Gonzalez (2007), Molecular ion composition measurements in the F1 region at Arecibo, *J. Geophys. Res.*, *112*, A06322, doi:10.1029/2006JA012028.
- Barth, C. A., D. W. Rusch, and A. I. Stewart (1973), The UV nitric-oxide experiment for Atmosphere Explorer, *Radio Sci.*, *8*, 379.

- Brace, L. H., R. F. Theis, and A. Dalgarno (1973), The cylindrical electrostatic probes for Atmosphere Explorer-C, -D, and -E, *Radio Sci.*, *8*, 341.
- Brace, L. H., and R. F. Theis (1978), An empirical model of the interrelationship of electron temperature and density in the daytime thermosphere at solar minimum, *Geophys. Res. Lett.*, *5*, 275.
- Brinton, H. C., L. R. Scott, M. W. Pharo III, and J. T. Coulson (1973), The Bennett ion-mass spectrometer on Atmosphere Explorer-C and -E, *Radio Sci.*, *8*, 323.
- Danilov, A. D., and V. K. Semenov (1978), Relative ion composition model at midlatitudes, *J. Atmos. Terr. Phys.*, *40*, 1093.
- Danilov, A. D., and N. V. Smirnova (1995), Improving the 75 to 300 km ion composition model of the IRI, *Adv. Space Res.*, *15*(2), 171.
- Deng, Y., and A. J. Ridley (2007), Possible reasons for underestimating Joule heating in global models: E field variability, spatial resolution, and vertical velocity, *J. Geophys. Res.*, *112*, A09308, doi:10.1029/2006JA012006.
- Hanson, W. B., D. Zuccaro, C. R. Lippincott, and S. Sanatani (1973), The retarding potential analyzer on Atmosphere Explorer, *Radio Sci.*, *8*, 333.
- Hierl, P. M., I. Dotan, J. V. Seeley, J. M. Van Doren, R. A. Morris, and A. A. Viggiano (1997), Rate constants for the reactions of O<sup>+</sup> with N<sub>2</sub> and O<sub>2</sub> as a function of temperature (300–1800 K), *J. Chem. Phys.*, *106*(9), 3540.
- Hoffman, J. H., W. B. Hanson, C. R. Lippincott, and E. E. Ferguson (1973), The magnetic ion-mass spectrometer on Atmosphere Explorer, *Radio Sci.*, *8*, 315.
- Nicolls, M. J., M. N. Vlasov, M. C. Kelley, and G. G. Shepherd (2006), Discrepancy between the nighttime molecular ion composition given by the International Reference Ionosphere model and airglow measurements at low latitudes, *J. Geophys. Res.*, *111*, A03304, doi:10.1029/2005JA011216.
- Nier, A. O., W. E. Potter, D. R. Hickman, and K. Mauersberger (1973), The open-source neutral-mass spectrometer on Atmosphere Explorer-C, -D and -E, *Radio Sci.*, *8*, 271.
- Picone, J. M., A. E. Hedin, D. P. Drob, and A. C. Aikin (2002), NRLMSISE-00 empirical model of the atmosphere: Statistical comparisons and scientific issues, *J. Geophys. Res.*, *107*(A12), 1468, doi:10.1029/2002JA009430.
- Richards, P. G. (2001), Seasonal and solar cycle variations of the ionospheric peak electron density: Comparison of measurement and models, *J. Geophys. Res.*, *106*, 12,803.
- Richards, P. G. (2002), Ion and neutral density variations during ionospheric storms in September 1974: Comparison of measurement and models, *J. Geophys. Res.*, *107*(A11), 1361, doi:10.1029/2002JA009278.
- Richards, P. G. (2004), On the increases in nitric oxide density at midlatitudes during ionospheric storms, *J. Geophys. Res.*, *109*, A06304, doi:10.1029/2003JA010110.
- Richards, P. G., and D. G. Torr (1983), A simple theoretical model for calculating and parameterizing the ionospheric photoelectron flux, *J. Geophys. Res.*, *88*, 2155.
- Richards, P. G., J. A. Fennelly, and D. G. Torr (1994), EUVAC: A solar EUV flux model for aeronomic calculations, *J. Geophys. Res.*, *99*, 8981.
- Richards, P. G., M. J. Nicolls, C. J. Heinselman, J. J. Sojka, J. M. Holt, and R. R. Meier (2009), Measured and modeled ionospheric densities, temperatures, and winds during the international polar year, *J. Geophys. Res.*, *114*, A12317, doi:10.1029/2009JA014625.
- Siscoe, G., D. Baker, R. Weigel, J. Hughes, and H. Spence (2004), Roles of empirical modelling within CISM, *J. Atmos. Sol. Terr. Phys.*, *66*, 1481.
- Takeda, M., and T. Araki (1985), Electric conductivity of the ionosphere and nocturnal currents, *J. Atmos. Terr. Phys.*, *47*, 601.
- Vlasov, M. N., M. J. Nicolls, M. C. Kelley, S. M. Smith, N. Aponte, and S. A. González (2005), Modeling of airglow and ionospheric parameters at Arecibo during quiet and disturbed periods in October 2002, *J. Geophys. Res.*, *110*, A07303, doi:10.1029/2005JA011074.
- Watari, S., I. Iwamoto, K. Igarashi, M. Isogai, and Y. Arakawa (2003), 3-D visualization of the IRI model, *Adv. Space Res.*, *31*(3), 781.

D. Bilitza, Department of Computational and Data Sciences, George Mason University, Fairfax, VA 22030, USA.

P. G. Richards and D. Voglozin, Department of Physics and Astronomy, George Mason University, Fairfax, VA 22030, USA. (pricharl@gmu.edu)